K. Sidi Ali, *et al.*: Thermal-hydraulic Behavior of Physical Quantities at Critical ...
Nuclear Technology & Radiation Protection: Year 2012, Vol. 27, No. 3, pp. 229-238

229

THERMAL-HYDRAULIC BEHAVIOR OF PHYSICAL QUANTITIES AT CRITICAL VELOCITIES IN A NUCLEAR RESEARCH REACTOR CORE CHANNEL USING PLATE TYPE FUEL

by

Kamel SIDI ALI [1*], *Zaki BOUDALI* [2], *and Rachid SALHI* [2]

[1]Division of Nuclear Safety and Radiation Protection, Nuclear Research Center of Draria, Draria, Algiers, Algeria
[2]Department of Mechanical Engineering, M. Polytechnic School, EMP, Bordj El-Bahri, Algiers, Algeria

The thermal-hydraulic study presented here relates to a channel of a nuclear reactor core. This channel is defined as being the space between two fuel plates where a coolant fluid flows. The flow velocity of this coolant should not generate vibrations in fuel plates. The aim of this study is to know the distribution of the temperature in the fuel plates, in the cladding and in the coolant fluid at the critical velocities of Miller, of Wambsganss, and of Cekirge and Ural. The velocity expressions given by these authors are function of the geometry of the fuel plate, the mechanical characteristics of the fuel plate's material and the thermal characteristics of the coolant fluid. The thermal-hydraulic study is made under steady-state; the equation set-up of the thermal problem is made according to El Wakil and to Delhaye. Once the equation set-up is validated, the three critical velocities are calculated and then used in the calculations of the different temperature profiles. The average heat flux and the critical heat flux are evaluated for each critical velocity and their ratio reported. The recommended critical velocity to be used in nuclear channel calculations is that of Wambsganss. The mathematical model used is more precise and all the physical quantities, when using this critical velocity, stay in safe margins.

Key words: nuclear reactor, reactor core, reactor channel, fuel plate, critical velocity, heat flux

INTRODUCTION

Fuel plates are typically used in light water nuclear reactors with low operating temperatures. The study presented here deals with a thermal-channel of a nuclear reactor core. This channel is defined as the space between two fuel plates where the coolant flows in order to remove heat. To extract this heat and to avoid disturbing the integrity of the fuel, which is a criterion of nuclear safety, we have to know the temperature distribution in the fuel, in the fuel cladding and in the cooling fluid. In fact the flow is summarized in the flow of water between two flat plates with a given velocity. Calculation of this velocity is based on two criteria: the first is the visibility and the second the critical velocity which should not be reached. The first expression for the critical velocity was established by Miller [1], it is given according to the density of the fluid, the geometry of the fuel and Young's modulus of the material used. Another expression was established by Wambsganss [2], which uses the same variables used by Miller [1] and adds some others to consider the

mathematical formulation. A third expression was proposed by Cekirge and Ural [3], which is somewhat simpler and does not require many calculations, it considers more of a relationship between material and fluid. Kerboua *et al.*, [4] studied the critical velocity induced by a potential flow on a plate. They developed a finite element method to model plates and plate systems with arbitrary boundary conditions subjected to forces induced by the passage of a potential fluid flow. The method used is the hybrid method combining the finite element method with the classical theory of thin plates. In this method, the fluid pressure on the structure is expressed in terms of the inertia of the fluid of the Coriolis force and centrifugal force. They found that for low heights of fluid, the clamped-free plate is most vulnerable to relative static instability compared to the plate clamped-clamped.

Cui *et al.*, [5] studied the vibration and the stability induced by the flow on a model of fuel element assemblies containing parallel plates, in order to solve the equations of the complex mode-modal. To do this, they used the method of variation of frequency. The results are subject of the design of fuel elements for nuclear re-

---

* Corresponding author; e-mail: kamelsidiali@gmail.com

230

K. Sidi Ali, *et al.*: Thermal-hydraulic Behavior of Physical Quantities at Critical ...
Nuclear Technology & Radiation Protection: Year 2012, Vol. 27, No. 3, pp. 229-238

actors and nuclear safety. Fujimura and Kelly [6] studied the linear stability of shear flow instability between two horizontal parallel plates. They were able to solve the eigenvalue problem numerically by using the expansion method of Chebyshev polynomials. They found that the critical Rayleigh number increases to two-dimensional disturbances with increasing Reynolds number. The result strongly supports the previous stability analysis and in some cases, a discontinuity in the critical wave number occurs due to the development of two extrema in the limit of neutral stability.

Tang and Paidoussis (2007) [7] treated the dynamics of a plate subjected to an axial flow on both surfaces. They have built a numerical model relatively simple to control and monitor the volatility of the post-critical behavior of the fluid-structure system by developing a nonlinear equation of motion of the plate using the inextensible condition. The analysis of the dynamics of the system was performed in the time domain. They found that various factors can affect the dynamics of the system such as damping materials, the length of the current segment and the viscous drag. Hence, they proposed a model of evolution wake to explain the phenomenon of hysteresis observed in experiments. Michelina and Llewellyn Smith [8] studied the linear stability of N identical flexible plates with boundary conditions (uniform parallel flow). Where the flow viscosity is neglected and the flow around the plates is assumed potential. A Galerkin method is used to calculate the eigenmodes of the system. Their interest was about the effects of the number of plates and their distance from the stability property in the static state. In this work, we seek to know the developments of different temperatures and the evolution of the critical heat flux for each of the three expressions for the critical velocity. Such information will contribute to exact dimensioning of the active part of the nuclear reactor core.

**THE CONCEPT OF
CRITICAL VELOCITY**

Miller, Wambsganss, and Cekirge and Ural use the equation of conservation of momentum of a continuous flat plate, elastic, isotropic and built at the lateral sides, subjected to longitudinal vibrations under the effect of fluid flow, incompressible and inviscid on its faces. The basic equation of the bending of a flat plate is given by

$$D \nabla^2 \nabla^2 w + \rho_m c \frac{\partial^2 w}{\partial t^2} = \Delta p(t) \qquad (1)$$

where

$$\Delta p(t) = p_2 - p_1 = \frac{1}{2} \rho_f A_0 U^2 \left(\frac{1}{A_1^2} - \frac{1}{A_2^2} \right) \qquad (2)$$

and

$$D = \frac{Ec^3}{12(1-v^2)} \qquad (3)$$

where w is the deflection of the plate, A_0 – the section out channel, A_1 – the section of channel 1, A_2 – the section of channel 2, t – the time, U – the input fluid velocity, ρ_f – the fluid density, ρ_m – the density of the material plate, p_1 – the local pressure on the face of channel 1, p_2 – the local pressure on the face of channel 2, D – the rigidity of the flexion, c – the thickness of the plate, and v – the Poisson ratio.

In fig. 1, front view and right view of the disposition of fuel plates are presented. In this figure Z represents the axis of the longitudinal arrow and X the axis of the transverse arrow. In that case, the arrow is according to the axis X, the eq. (1) becomes

$$D \frac{\partial^4 w}{\partial x^4} + \rho c \frac{\partial^2 w}{\partial t^2} = \Delta p(t) \qquad (4)$$

**CRITICAL VELOCITY
MODELS AND EQUATION SET UP**

Miller and Wambsganss build their model based on a single plate. The difference between the two models is that the former considers only the first order terms of the equation for approximating the pressure gradient, while the second takes into account, in addition to the terms of the first order, the terms of the second order. This is presented in the following two points:
– Miller considers only first order terms in his study. The distribution of the cross-section is written as

$$A_1(w,t) = \int_0^a (H - 2w)\mathrm{d}x \qquad (5)$$

$$A_2(w,t) = \int_0^a (H - 2w)\mathrm{d}x \qquad (6)$$

where H is the thickness of the channel. The pressure gradient after a Taylor series expansion is given by
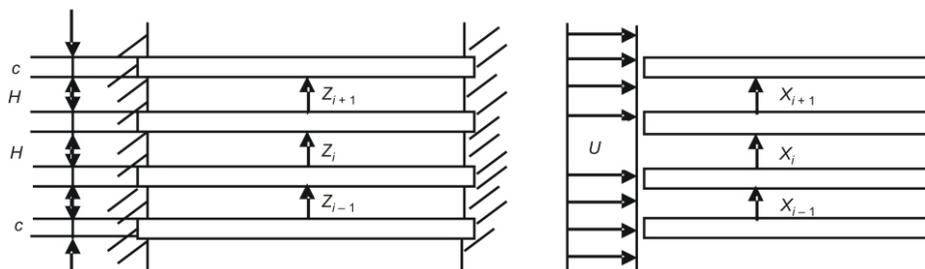

Figure 1. Views of the cross-section of a fuel plate assembly

$$\Delta p(t) \quad \frac{\rho_f A_0 U^2}{H} z \qquad (7)$$

– Wambsganss considers, in addition to the terms of the first order, second order ones

$$\Delta p(t) \quad \frac{\rho_f A_0 U^2}{H} z \; 1 \; \frac{8}{H^2} z^2 \qquad (8)$$

with

$$z \quad \frac{1}{a} \int_0^a w \, dx \qquad (9)$$

The model used by Cekirge and Ural is based on the same assumptions as those made by Miller and Wambsganss. The authors use the basic eq. (4) of the bending of flat plates in order to build a system of partial differential equations that meets the linearity requirements and satisfies the conditions of the resolution by the method of Galerkin. As the flow is incompressible and potential, we obtain the equation of velocity potential in the channel i

$$\frac{\partial^2 \phi_i}{\partial x_i^2} \quad \frac{\partial^2 \phi_i}{\partial y_i^2} \quad \frac{\partial^2 \phi_i}{\partial z_i^2} \quad 0 \qquad (10)$$

RESOLUTION

Model of Miller and Wambsganss

Miller and Wambsganss used the method of separation of variables by representing the arrow as the product of two functions, the one depends on the position and the other one depends on time to extract the first appropriate frequency of the plate

$$w(x,t) \quad \psi(x) T(t) \qquad (11)$$

where $T(t)$ is the generalized coordinate and $\psi(x)$ is the fundamental normal mode which satisfies

$$\frac{d^4 \psi}{dx^4} \quad \lambda^4 \psi \qquad (12)$$

where λ is a constant proportional to the frequency of the structure. The method of Galerkin is applied by substituting eqs. (7)-(9) and by using eq. (11) in eq. (4). After integration, following x, between 0 and a, we obtain the equation

$$T \quad M^2 T \quad N^2 T^3 \quad 0 \qquad (13)$$

where

$$M^2 \quad \frac{1}{\mu} \sqrt{\lambda^4 \; K \; \frac{\int_0^1 \psi(\bar{x}) \; \int_0^1 \psi(\bar{x}) d\bar{x} \; d\bar{x}}{\int_0^1 \psi^2(\bar{x}) d\bar{x}}}$$

$$N^2 \quad \frac{1}{\mu H} \sqrt{8K \; \frac{\int_0^1 \psi(\bar{x}) \; \int_0^1 \psi(\bar{x}) d\bar{x}^3 \; d\bar{x}}{\int_0^1 \psi^2(\bar{x}) d\bar{x}}}$$

where μ, K, and $\bar{x}$ are constants given by

$$\mu^2 \quad \frac{\rho c}{D}, \quad K \quad \frac{4\rho_f V_0^2}{DH}, \quad \bar{x} \quad \frac{x}{a}$$

Equation (12) has to be stable, so it is necessary that

$$M^2 \quad 0 \text{ and } |T| \quad \left|\frac{M}{N}\right| \qquad (14)$$

In the case where the terms of the first order (work of Miller) are taken into account, it is enough to verify just the first condition because the second one is always insured because $N = 0$

$$\lambda^4 \quad K \; \frac{\int_0^1 \psi(\bar{x}) \; \int_0^1 \psi(\bar{x}) d\bar{x} \; d\bar{x}}{\int_0^1 \psi^2(\bar{x}) d\bar{x}}$$

$$v_0 \quad v_{CR} \quad \sqrt{\alpha \frac{Ec^2 H}{(1 \; v^2) \rho_m a^4}} \qquad (15)$$

where

$$\alpha \quad \frac{(\lambda a)^4 \int_0^1 \psi^2(\bar{x}) d\bar{x}}{48 \int_0^1 \psi(\bar{x}) \; \int_0^1 \psi(\bar{x}) d\bar{x} \; d\bar{x}} \qquad (16)$$

With v_0, the fluid velocity in the channel and α a constant depending on the mode of plate fixation, on the appropriate frequency and on the width of the plate. If the second order is considered, it is necessary to verify also the second condition on the generalized coordinate.

$$\delta(t) \quad \psi_{max} T(t) \qquad (17)$$

Using eq. (17) to rewrite the second condition

$$|\delta| \quad \psi_{max} \left|\frac{M}{N}\right| \qquad (18)$$

The critical arrow is defined by

$$\delta_{CR} \quad \beta H \sqrt{\frac{v_{CR}}{v_0}^2 \; 1} \qquad (19)$$

where v_{CR} is the critical velocity of Miller and β is given by

$$\beta \quad \sqrt{\frac{\psi_{max}^2 \int_0^1 \psi^2(\bar{x}) d\bar{x}}{8 \int_0^1 \psi(\bar{x}) \; \int_0^1 \psi(\bar{x}) d\bar{x}^3 \; d\bar{x}}} \qquad (20)$$

We also define a coefficient of design k which is equal to the ratio of the critical arrow and the thickness of the channel

$$k \quad \frac{\delta_{CR}}{H} \qquad (21)$$

The new critical velocity given by Wambsganss is then written

$$V_{CR} \quad \gamma v_{CR} \qquad (22)$$

232

K. Sidi Ali, *et al*.: Thermal-hydraulic Behavior of Physical Quantities at Critical ...
Nuclear Technology & Radiation Protection: Year 2012, Vol. 27, No. 3, pp. 229-238

with

$$\gamma \quad \sqrt{1 \quad \frac{k}{\beta}^2} \tag{23}$$

Model of Cekirge and Ural

To use the model of Cekirge and Ural, one has to solve eq. 10. To do this, boundary conditions must be used on the arrow, fig. 2, and have to be verified
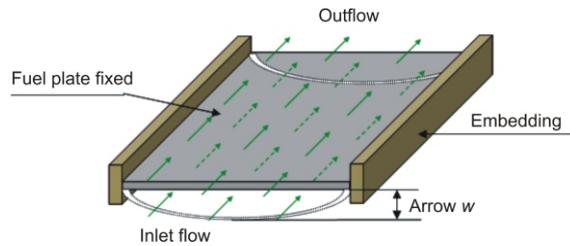

Figure 2. Mode of fixing of the fuel plate

$$w_i \quad x_i, \frac{a}{2}, t \quad w_i \quad x_i, \frac{a}{2}, t \quad 0 \tag{24}$$

$$\frac{\partial w_i}{\partial y_i} \quad x_i, \frac{a}{2}, t \quad \frac{\partial w_i}{\partial y_i} \quad x_i, \frac{a}{2}, t \quad 0 \tag{25}$$

where a is the width of the fuel plate. The arrow at the entrance and at the exit of the channel has finite values

$$w_i \quad \infty, \frac{b}{2}, t \quad w_i \quad \infty, \frac{b}{2}, t \quad \text{finite} \tag{26}$$

where b is the length of the channel.

The deflection can be selected taking into account the three previous conditions, eqs. (24)-(26) as

$$w_i \quad w_i^0 \quad 1 \quad \cos \frac{2\pi y_i}{b} \quad \exp[i(\omega t \quad kx_i)] \tag{27}$$

where ω, k, and w_i^0 are the frequency, the wave number and a constant, respectively, and i is the complex number such that: $(i^2 = -1)$. The velocity potential is written as

$$\phi_i \quad \phi_{i0}(y_i, z_i) \exp[i(\omega t \quad kx_i)] \tag{28}$$

The boundary conditions for the velocity potential are

$$\left.\frac{\partial \phi_i}{\partial y_i}\right|_{y_i \quad 0} \quad \left.\frac{\partial \phi_i}{\partial y_i}\right|_{y_i \quad \mp b/2} \quad 0 \tag{29}$$

$$\left.\frac{\partial \phi_i}{\partial z_i}\right|_{z_i \quad 0} \quad \frac{\partial w_i}{\partial t_i} \quad U \frac{\partial w_i}{\partial x_i} \tag{30}$$

$$\left.\frac{\partial \phi_i}{\partial z_i}\right|_{z_i \quad d} \quad \frac{\partial w_i \quad 1}{\partial t_i} \quad U \frac{\partial w_i \quad 1}{\partial x_i \quad 1} \tag{31}$$

where U is the fluid velocity, at the channel entry, and d the channel thickness. ϕ_i is written as

$$\phi_i \quad \phi_{ia} \quad \phi_{ib} \tag{32}$$

The pressure distribution below and above the channel is determined by applying the Bernoulli equation

$$p_{1i} \quad \rho_f \quad \frac{\partial \phi_i}{\partial t} \quad U \frac{\partial \phi_i}{\partial x_i}\bigg|_{z_i \quad 0} \tag{33}$$

and

$$p_{2i} \quad \rho_f \quad \frac{\partial \phi_{i \quad 1}}{\partial t} \quad U \frac{\partial \phi_{i \quad 1}}{\partial x_i}\bigg|_{z_{i \quad 1} \quad d} \tag{34}$$

Substituting eqs. (27), (33), and (34) in eq. (4) by using eqs. (29)-(31), applying the Galerkin method, and integrating eq. (4) following x between 0 and a, one obtains

$$Aw_{i \quad 1}^0 \quad Bw_i^0 \quad Aw_{i \quad 1}^0 \quad 0 \tag{35}$$

where

$$A \quad \frac{\mu(U^* \quad C^*)^2}{2\pi} \quad \frac{1}{b} \sinh \quad 2\pi e \frac{b}{l}$$

$$\frac{1}{2}\sqrt{1 \quad \frac{b^2}{l^2}} \sinh \quad 2\pi e \quad 1 + \frac{b^2}{l^2}^2 \tag{36}$$

$$B \quad \frac{1}{4} \quad \frac{2}{3} \quad \frac{2b}{l}^2 \quad 4 \quad 8 \quad \frac{L}{2b}^2 \quad \frac{3C^{*2}}{2} \quad D \tag{37}$$

$$D \quad \frac{\mu(U^* \quad C^*)^2}{\pi} \quad \frac{l}{b} \text{tgh} \quad 2\pi e \frac{b}{l}$$

$$\frac{1}{2}\sqrt{1 \quad \frac{b^2}{l^2}} \text{tgh} \quad 2\pi e \quad 1 \quad \frac{b^2}{l^2} \tag{38}$$

with l the wave length of the perturbation, $k = 2 /l$, $\omega = 2 \ C/l$, $\mu = \rho b/\rho_m h$, $U^* = U/C_0$, $C^* = C/C_0$, C the wave velocity, $C_0 = 2(D/\rho_m hb^2)^{1/2}$, $e = d/b$ and $\omega_0 = C_0/b$.

For m plates with recessed edges, we assemble the following system

$$\Delta w^0 = 0 \tag{39}$$

where Δ is the matrix of dimension $(m \quad m)$ and w^0 the modal vector of m elements

$$\Delta w^0 \quad \begin{matrix} B & A & 0 & . & . & 0 & w_1^0 \\ A & B & A & . & . & . & w_2^0 \\ 0 & A & B & . & . & . & . \\ . & . & . & B & A & 0 & . \\ . & . & . & A & B & A & w_{m-1}^0 \\ 0 & . & . & 0 & A & B & w_m^0 \end{matrix} \tag{40}$$

To have a solution that is non-trivial, it requires that the determinant of this system is zero

$$\det(\Delta) \quad D_m \quad B D_{m \quad 1} \quad A^2 D_{m \quad 2} \quad 0 \tag{41}$$

as $D_1 = B$ and $D_2 = B^2 - A^2$

To solve eq. (39), one uses an iterative method and obtains the expression for C^*

$$C_1^{*2} \quad \frac{A^2 D_{m \quad 2}(C_0^{*2})}{b_2 D_m(C_0^{*2})} \quad \frac{b_1}{b_2} \tag{42}$$

To calculate the dimensionless parameter C^* corresponding to the first eigenmode that satisfies eq. (41), we have to determine first the wavelength $l = b/2$, because the plate is recessed on both sides, one has just to get the first eigenmode and then do iterations on C* until the convergence of the calculations.

THERMAL EQUATION SET UP

To calculate the heat transfer in a nuclear reactor core channel one uses El-Wakil [9] and Delhaye [10] equation set up. This equation set up was used by Khedr [11] and it gave good results. The same approach is applied here after. At steady state, the heat generated in the fuel is transferred to the coolant through the clad. The temperature distribution of the coolant in the axial channel (*i*)

$$T_f(i, z) \quad T_{fl} \quad 0.001 \frac{q_c(i) A_m l_e}{\pi C_p m_{ch}} \quad \sin \frac{\pi z}{l_e} \quad \sin \frac{\pi l_h}{2l_e} \tag{43}$$

The distribution of the axial temperature of the clad T_c into the channel (*i*) is

$$T_c(i, z) \quad T_f(i, z) \quad \frac{q_c(i) t_m}{2h(i)} \cos \frac{\pi z}{l_e} \tag{44}$$

The axial temperature distribution of the meat, in the channel *I*, is

$$T_m(i, z) \quad T_c(i, z) \quad q_c(i) \cos \frac{\pi z}{l_e} \quad \frac{t_m^2}{8k_m} \quad \frac{t_m t_c}{2k_c} \tag{45}$$

where A_c is the cross-section of the channel, A_m – the cross-section of the meat, C_p – the specific heat of coolant, H – the channel thickness, l_h – the active length of the plate or fuel heated channel length, m_{ch} – the mass flow, t_c – the thickness of the clad, t_m – the thickness of the meat, w_m – the width of the meat, z – the axial location of the channel which is equal to zero at the center of the channel, and T_{fl} – the inlet temperature based coolant. We note that the maximum power density in the channel is given by

$$q_c(i) \quad F(i) q_a \tag{46}$$

As q_c is the average power density base which is the base power divided by the volume of fuel and $F(i)$ – the factor of nuclear power. The mass flow m_{ch} and the velocity of the channel V_{ch} are given by

$$m_{ch} \quad \frac{F_d W_T \rho_f}{FPTN} \tag{47}$$

$$V_{ch} \quad \frac{m_{ch}}{\rho_f A_{ch}} \tag{48}$$

where A_{ch} is the transverse section of the channel, $FPTN$ – the total number of fuel plates, F_d – a factor less than unity ($F_d = 0.9$), W_T – the total volume flow, and ρ_f – the density of fluid.

HEAT FLUX AND CRITICAL HEAT FLUX IN A CHANNEL

When flowing in the channel, the water warms up, thus T_f increases as well as the temperature of the clad. If in a point, this last one reaches the value T_{sat}, bubbles of steam will appear: It is the local boiling. In this region, the average temperature T_f of the water remains below T_{sat}. The first correlation giving the heat flux was established by Mc Adams *et al.* [12] valid for low pressure, less than 0.63 MPa. Another correlation was given by Jens and Lottes [13], valid for pressure less than 14 MPa. Another correlation valid for high pressure was given by Thom [14]. In this study, the correlation developed by Bergeles and Rohsenow [15], applicable for low pressures characteristic of research reactors, is used.

After this, the bubbles become larger in the liquid and unite in a nucleus gaseous which leaves place for a liquid annular flow. This last one aims to disappear with the continuous coming of heat through the solid wall: there is a drying region where the burnout can happen, Bernard [16]. In the area of nucleate boiling, if the heat flow exceeds a given critical value q_{cr}, a steam film is formed on the surface of the clad and we have the phenomenon of the boiling crisis. Typically, this situation has to be avoided because the heat transfer coefficient falls sharply. The heat produced in the fuel will be badly evacuated. It follows an increase in temperature in the core of the plates which can lead to the fusion of fuel. The critical heat flux can be calculated by the correlation established by Bernath [17] valid for high pressure and high fluid velocity. For low pressure and low fluid velocity, the correlation of Sudo *et al.* [18] is recommended. One can find in the literature more correlations. In this work two correlations will be used, the one of Mirshak *et al.* [19] and that of Labunstov [20]. The expressions giving the heat flux and the critical heat flux are presented in tab. 4.

The critical heat flux ratio is the ratio of the critical heat flux and the heat flux in the core. The margins of nuclear reactor safety require that this ratio should at least be equal to 1.3 for proper reactor operation. The ratio of the critical heat flux or RFTC is given by

$$RFTC \quad \frac{q_{cr}(i, z)}{q(i, z)} \tag{49}$$

This ratio allows knowing the situation with respect to the risk of burnout. It passes through a minimum at a critical height. Indeed, it must be, held far enough from the boiling crisis that could damage the fuel plates.

APPLICATION AND RESULTS

To know the thermal hydraulic performance, of a nuclear reactor whose flow is driven at a critical veloc-

234

K. Sidi Ali, *et al.*: Thermal-hydraulic Behavior of Physical Quantities at Critical ...
Nuclear Technology & Radiation Protection: Year 2012, Vol. 27, No. 3, pp. 229-238

Table 1. Dimensions and characteristics of the 10 MW nuclear reactor, TECDOC-233 (1980) [21]

Property	10 MW	Property	10 MW
No. of standard fuel elements (SFE)	23	No. of plates in SFE	23
No. of control fuel elements (CFE)	5	No. of plates in CFE	17
Channel heated width [cm]	6.64	Plate total length [cm]	62.5
Channel heated width [cm]	6.3	Channel thickness [cm]	0.219
Fuel plate heated length [cm]	60	Clad thickness [cm]	0.038
Core inlet temperature [°C]	38	Meat thickness [cm]	0.051
Core exit pressure (bar absolute)	1.566	Radial power factor	1.78
Clad thermal conductivity [Wm^{-1}°C^{-1}]	180	Axial power factor	1.4
Meat thermal conductivity [Wm^{-1}°C^{-1}]	53.6	Total core flow [mh^{-1}]	1000
		Channel velocity [ms^{-1}]	2.97

Table 2. Constant dependent binding mode [1]

Deflection	Longitudinal		Transverse	
Edge fixies	α	β	α	β
Pinned	2.03	0.409	2.5	0.616
Fixed	10.42	0.414	**15.1**	**0.814**
Cantilever	0.258	0.450	–	–

Table 3. Properties of the material [1]

Type of cladding material	Characteristics	
	Young's modulus [GPa]	100
Aluminum alloy of nuclear grade	Poisson coefficient	0.34
	The density [kgm^{-3}]	20 10^3
	The design coefficient	0.5

One will plot the temperature profiles to see how the changes are in the fluid temperature at the exit of the nuclear reactor core and the limits of the temperature of the cladding, this on one hand. On the other hand, we check the limit of the critical flow for the proper functioning of the nuclear reactor core. In tabs. 2 and 3, the binding modes of the plates and the properties of the cladding material are presented.

FLUX CALCULATION AT THE ONSET OF NUCLEATE BOILING AND CRITICAL HEAT FLUX

To check the safety of the nuclear reactor core from the ONB, Onset of nucleate Boiling, it is necessary to calculate the critical flux and the average flux. In tab. 4, the values of average heat flux and critical

ity, an application is made for a 10 MW nuclear reactor, the dimensions and characteristics of this nuclear reactor are given in tab. 1 from TECDOC-233 [21].

Table 4. Flux values calculated and those given in TECDOC-233 (1980) [21]

Flux	Correlation	10 MW
Q_{av} [Wcm^{-2}]	The correlation of Bergles and Rohsenow: $$Q_{av} = \dfrac{T_{sat} - T_{f1} - \dfrac{5}{9}\,\dfrac{9.23 F Q_{av}}{p^{1.156}}\,\dfrac{p^{0.0284}}{216}}{\dfrac{2\,10^5\, F r L_h W_m}{\rho V_{ch} H C_p W_\varepsilon}\,\dfrac{100 F}{h}}$$ Iterative computation (fixed point method)	Present study 32.11
		Ref. [21]: 35.9
Q_{cr} [Wcm^{-2}] $T_{sat} = 100$ °C $T_{fl} = 38$ °C $P = 1$ bar	The correlation of Mirshak *et al.* $$Q_{cr} = \dfrac{151(1 - 0.01112 V_{ch})[1 - 0.00914(T_{sat} - T_{fl})](1 - 0.0009P)}{1 - \dfrac{27.6 L_h W_m}{\rho V_{ch} H C_p F d W_t}(1 - 0.01112 V_{ch})(1 - 0.0009P)}$$	Present study 247.91
		Ref. [21]: 266
	The correlation of Labuntsov $$Q_{cr} = \dfrac{145.5\theta(P)\left(1 - \dfrac{2.5 V_{ch}^2}{\theta(P)}\right)^{0.25}\left(1 - \dfrac{15.1 C_p (T_{sat} - T_{fl})}{\lambda P^{0.5}}\right)}{145.5\theta(P)\left(1 - \dfrac{2.5 V_{ch}^2}{\theta(P)}\right)^{0.25}\dfrac{15.1 C_p}{\lambda P^{0.5}}\dfrac{20 L_h W_m}{\rho V_{ch} H C_p W_\varepsilon}}$$ $$\theta(P) = 0.99531 P^{0.33}\left(1 - \dfrac{P}{P_{cr}}\right)^{1.33}$$	Present study 348.57
		Ref. [21]: 353

heat flux in the channel are calculated using different correlations for the 10 MW reactor. These fluxes are calculated using the same velocity channel given in tab. 1 and the obtained results are compared to those given in Tecdoc-233 [21].

The average flux difference between this study and reference [21] is of the order of 10.7%. The critical heat flux calculated with the correlation of Mirshak gives a relative difference of about 6.8% compared to the reference [21] and for the correlation of Labuntsov the difference is about 1.25%. The obtained results are acceptable compared to those given in reference [21]. Once this validation is done, the three critical velocities are calculated, in the case of the 10 MW nuclear reactor, and presented in tab. 5.

Table 5. Calculated critical velocities

The power of the core	10 MW		
Critical velocities [ms^{-1}]	Miller	Wambsganss	Cekirge at Ural
	10.48	8.38	4.78

TEMPERATURE PROFILES AT CRITICAL VELOCITIES

The temperature profiles calculated using the three critical velocities are presented in figs. 3-5.

Figure 3 shows the temperature profile of the coolant in the channel for the three values of the critical velocity, that of Miller, that of Wambsganss and that of Cekirge and Ural. In the three cases, we notice that the inlet fluid temperature is 40 °C and it is constant for the three cases. The temperature of the fluid increases along the channel. The temperature of the fluid at the exit of the channel is respectively: 44.781 °C using Miller critical velocity, 45.976 °C using Wambsganss critical velocity and 50.566 °C using Cekirge and Ural critical velocity. It is clear that the outlet temperature of the coolant using the critical ve-
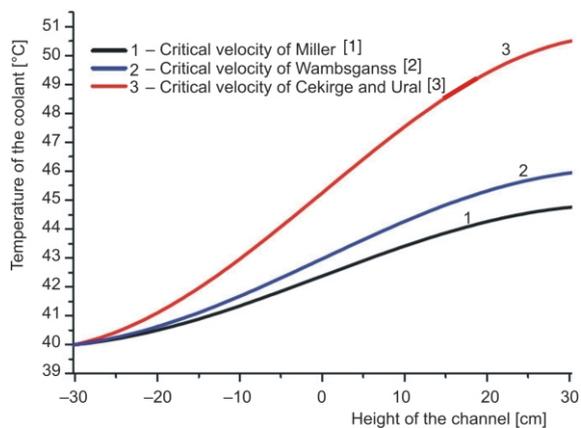

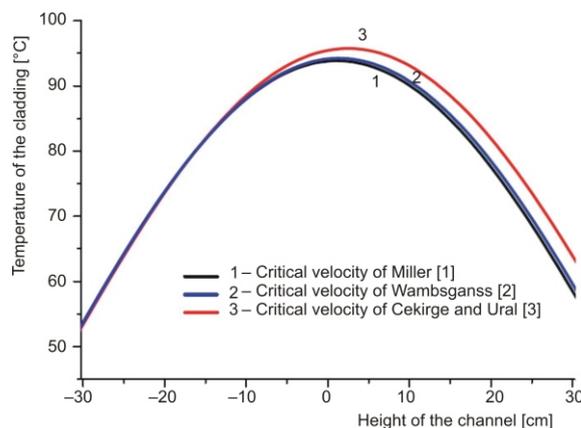**Figure 3. Temperature profiles of the fluid at critical velocities**

Figure 4. Temperature profiles of the clad at critical velocities
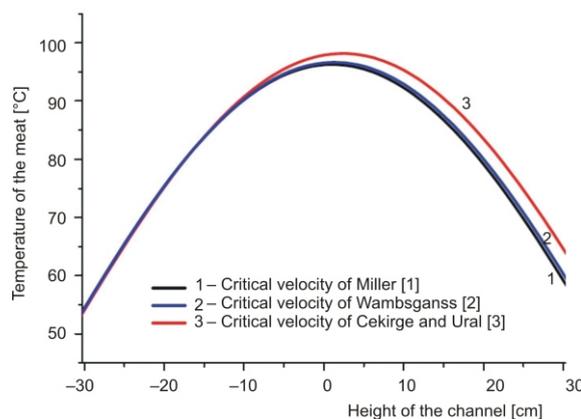

Figure 5. Temperature profiles of the meat at critical velocities

locity of Cekirge and Ural exceeds that of Miller and that of Wambsganss.

In fig. 4 the profiles of the temperature in the clad for the three critical velocities are presented. The calculated temperatures of the clad at the entrance of the channel using the critical velocity of Miller, that of Wambsganss and that of Cekirge and Ural are 51.021 °C, 50.96 °C, and 50.721 °C, respectively, the clad temperature increases until a maximum value for the three cases. The peak values using the critical velocity of Miller and the one for Wambsganss are 93.851 °C and 94.229 °C, respectively, located at 1.25 cm from the center of the channel and 95.749 °C located at 2.5 cm from the center of the channel when using Cekirge and Ural critical velocity. The very hot point of the channel is situated at these peaks. One observed that the peak temperature moves toward the center of the channel when the fluid velocity increases. So we can say that the peak position is inversely proportional to the velocity of the coolant. After these peaks, the temperature of the clad, for the three critical velocities, decreases until the exit of the channel and the values are:

236

K. Sidi Ali, *et al*.: Thermal-hydraulic Behavior of Physical Quantities at Critical ...
Nuclear Technology & Radiation Protection: Year 2012, Vol. 27, No. 3, pp. 229-238

55.834 °C, 56.976 °C, and 61.359 °C, respectively, using critical velocity of Miller, Wambsganss, and Cekirge and Ural. The last remark is about the clad temperature using the critical velocity of Cekirge and Ural: the clad is hotter because of the smallest critical velocity used and then less heat is transferred compared to the case when the two other critical velocities are used.

In fig. 5 the profiles of the meat temperature for three critical velocities are presented. At the entry of the channel, the calculated meat temperatures are 51.53 °C, 51.478 °C, and 51.24 °C, respectively, when using the critical velocity of Miller, that of Wambsganss and that of Cekirge and Ural. For the three critical velocities, the temperature increases until a maximum of 96.258 °C and 96.636 °C located at 1.25 cm from the center of the channel when using the critical velocity of Miller and that of Wambsganss, respectively. In the case of the use of the critical velocity of Cekirge and Ural, the temperature peak is 98.145 °C and it is located at 2.5 cm from the center of the channel. The three peaks are the points where the meat is very hot. It is found, as for the clad temperature that the peak temperature moves toward the center of the channel when the fluid velocity increases. The same conclusion as for the clad is made about the proportionality between the peak position and the coolant velocity. After these peaks, the temperature decreases in the channel until the exit and it is 56.353 °C, 57.494 °C, and 61.877 °C, respectively, when using the critical velocity of Miller, that of Wambsganss, and that of Cekirge and Ural.

In fig. 6 the profiles of the critical heat flux along the channel when using the critical velocity of Miller, that of Wambsganss and that of Cekirge and Ural are presented. The critical heat flux decreases along the channel for all critical velocities. This is due to the increase of the coolant temperature along the channel. The critical heat flux profile calculated using the critical velocity of Cekirge and Ural is the lowest one. Because of these lowest values, nucleate boiling can be achieved and it can easily occur. When using the two
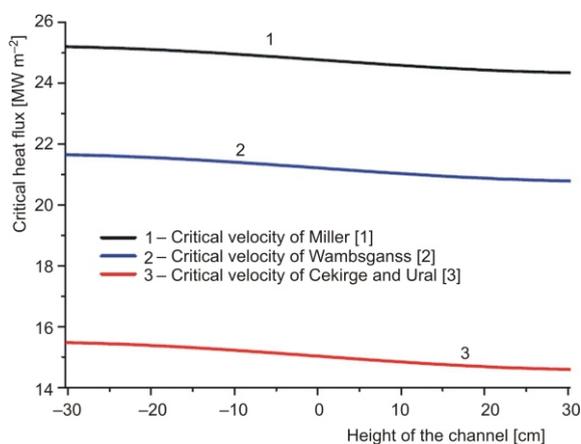

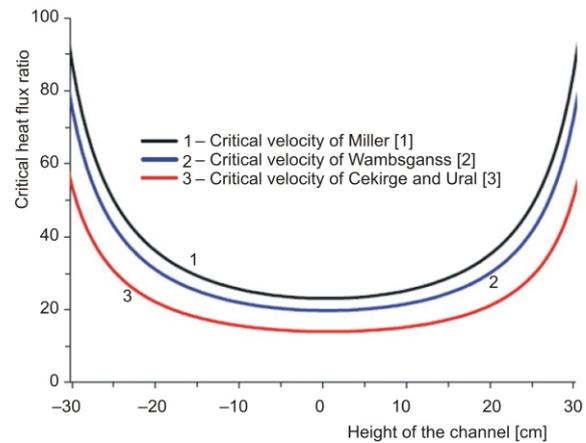**Figure 6. Critical heat flux profiles at critical velocities**

Figure 7. Critical heat flux ratio profiles at critical velocities

other critical velocities, the critical heat flux is raised by about 40% to 50% and ensures a more safe behavior.

The profiles of the critical heat flux ratio are presented in fig. 7 when using the three critical velocities. The interesting thing in each profile is the minimum critical heat flux ratio reached. This ratio is about 23.076, 19.760, and 13.989 when using, respectively, the critical velocity of Miller, that of Wambsganss and that of Cekirge and Ural. These ratios are situated at 0.625 cm from the center of the channel. The three ratio values are greater than 1.3, so they are sufficiently far from the boiling crisis that could merge the fuel cladding plates

CONCLUSIONS

To increase the coolant velocity in a channel of a nuclear reactor core, using fuel plates, one has to choose the best critical velocity model. In this work three critical velocities were presented, developed and resolved. The equation setup was validated on a 10 MW nuclear reactor using fuel plates. To see the effect of each of the critical velocities on the heat transfer in the channel, the temperature profiles of meat, clad and coolant were plotted. The average heat flux and the critical heat flux were calculated and their ratio plotted. The three critical velocity models are the one of Miller, the one of Wambsganss, and the one of Cekirge and Ural. By analyzing the evolution of the thermal-hydraulic quantities towards these three velocities, one sees that by using the critical velocity of Cekirge and Ural an increase of the coolant temperature is made much higher than with the other two models. This model increases also the clad temperature and this presents a risk of reaching the melting point of the cladding material. Finally, it also increases the risk of having a boiling crisis. If the critical velocity of Miller is used, one is sure that all the quantities are safe. The model gives the highest value of the

K. Sidi Ali, *et al.*: Thermal-hydraulic Behavior of Physical Quantities at Critical ...
Nuclear Technology & Radiation Protection: Year 2012, Vol. 27, No. 3, pp. 229-238

237

critical velocity. This is over-estimated because of the mathematical model neglects the second order terms as presented. The use of Wambsganss critical velocity is recommended because the mathematical model is more precise, it takes into account the second order terms. One can compare the results obtained when using Miller's critical velocity or Wambsganss's one. For the coolant temperature, the relative difference is about 2.84 %. The relative difference is less than 1% for the clad or meat temperature. The ratio of the critical heat flux confirms that the Wambsganss critical velocity maintains all the thermal-hydraulic quantities in safe margins.

REFERENCES

[1] Miller, D. R., Critical Flow Velocities for Collapse of Reactor Parallel-Plate Fuel Assemblies, *ASME J. Eng., 82* (1960), 2, pp. 83-95

[2] Wambsganss, Jr. M. W., Second-Order Effects as Related to Critical Coolant Flow Velocities and Reactor Parallel Plate Fuel Assemblies, *Nuclear Engineering and Design, 5* (1967), 3, pp. 268-276

[3] Cekirge, H. M., Ural, E., Critical Coolant Flow Velocities in Reactors Having Parallel Fuel Plates, *Comp. and Maths with Appls, 4* (1978), 2, pp. 153-156

[4] Kerboua, Y., *et al.*, Critical Velocity Induced by a Potential Flow on a System of Plates, Polytechnic School of Montreal, Technical Report EPM-RT-2006-05

[5] Cui, Z. D., *et al.*, Flow-Induced Vibration and Stability of an Element Model for Parallel-Plate Fuel Assemblies, *Nuclear Engineering and Design, 238* (2008), 7, pp. 1629-1635

[6] Fujimura, K., Kelly, R. E., Stability of Unstably Stratified Shear Flow Between Parallel Plates, *Fluid Dynamics Research, 2* (1987), 4, pp. 281-292

[7] Tang, L., Paidoussis, M. P., On the Instability and the Post-Critical Behavior of Two-Dimensional Cantilevered Flexible Plates in axial Flow, *Journal of Sound And Vibration, 305* (2007), 1-2, pp. 97-115

[8] Michelin S., Llewellyn Smith, S.G., Linear Stability Analysis of Coupled Parallel Flexible Plates in an Axial Flow, *Journal of Fluids and Structures, 25* (2009), 7, pp. 1136-1157

[9] El-Wakil, M. M., Nuclear Heat Transport, International Text book Company, Cranton, Penn., USA, 1971

[10] Delhaye, J. M., Reactors Thermal-Hydraulics, Edition Diffusion Press Sciences, Les Ulis, France, 2008

[11] Khedr, A., Thermal-Hydraulic Fortran Program for Steady-State Calculations of Plate-Type Fuel Research Reactors, *Nucl Technol Radiat, 23* (2008), 1, pp. 19-30

[12] McAdams, W. H., *et al.*, Heat Transfer at High Rates to Water with Surface Boiling, *Ind. Eng. Chem., 41* (1949), 9, pp. 1945-1953

[13] Jens, W. H., Lottes, P. A., Analysis of Heat Transfer, Burnout, Pressure Drop and Density Data for High Pressure Water, Technical Report ANL-4627, 1951

[14] Thom, R. S., Boiling in Sub-Cooled Water During Flow up Heated Tubes or Annuli, Proc. Inst. Mech. Eng., Part C: *Journal of Mechanical Engineering Science, 180* (1965-1966), pt. 3C

[15] Bergles, A. E., Rohsenow, W. M., The Determination of Forced Convection Surface-Boiling Heat Transfers, Transactions of the ASME 86, Series C – *Journal of Heat Transfer, 86* (1964), 3, pp. 365-371

[16] Bernard, J., Nuclear Energy 2, Nuclear Reactors Electro-Generators, Ellipses Edition, Paris, France, 2008

[17] Bernath, L., A Theory of Local-Boiling Burnout and its Application to Existing Data, *Chem. Eng. Prog. Symp. Ser., 56* (1960), 30, pp. 95-11

[18] Sudo, Y., *et al.*, Experimental Study of Differences in DNB Heat Flux Between Up-Flow and Down-Flow in Vertical Rectangular cChannel, *J. Nucl. Sci. Technol., 22* (1985), 8, pp. 604-618

[19] Mirshak, S., Durant W. D., Towell R. H., Heat Flux at Burnout, Technical Report DP-355, 1959

[20] Labunstov, D. A., Critical Thermal Loads in Forced Motion of Water which is Heated to a Temperature Below the Saturation Temperature, *Soviet Journal of Atomic Energy (English Translation), 10* (1961), 5, pp. 516-518

[21] ***, TECDOC-233, Research Reactor Core Conversion from the Use of Highly Enriched Uranium to the Use of Low Enriched Uranium Fuels Guidebook, IAEA, 1980

238

K. Sidi Ali, *et al*.: Thermal-hydraulic Behavior of Physical Quantities at Critical ...
Nuclear Technology & Radiation Protection: Year 2012, Vol. 27, No. 3, pp. 229-238

Камел СИДИ АЛИ, Заки БУДАЛИ, Рашид САЛХИ

ТЕРМОХИДРАУЛИЧКО ПОНАШАЊЕ ФИЗИЧКИХ ВЕЛИЧИНА ПРИ КРИТИЧНИМ БРЗИНАМА У КАНАЛУ ЈЕЗГРА ИСТРАЖИВАЧКОГ НУКЛЕАРНОГ РЕАКТОРА СА ПЛОЧАСТИМ ГОРИВОМ

Термохидарулочка студија овде приказана тиче се једног канала у језгру нуклеарног реактора. Канал је дефинисан као простор између две плоче горива кроз који протиче хладилац. Брзина струјања хладиоца не би требало да генерише вибрације у горивним плочама. Циљ студије је да се одреди расподела температуре у горивним плочама, у кошуљици и у хладиоцу при критичним брзинама које су дефинисане у радовима других истраживача. Њихови изрази за брзине су функције геометрије горивне плоче, механичких карактеристика материјала у горивним плочама и термичких карактеристика хладиоца. Термохидрауличко проучавање обављено је за стационарно стање, а основне једначине термичког проблема преузете су из одговарајуће литературе. Пошто је систем једначина потврђен, три критичне брзине израчунате су и потом коришћене за прорачун различитих температурних расподела. Израчунати су средњи топлотни флукс и критични топлотни флукс за сваку критичну брзину и приказани су њихови односи. Одређена је критична брзина коју треба користити у прорачунима нуклеарног канала. Математички модел је довољно прецизан да све физичке величине израчунате са овом критичном брзином остају у сигурним границама.

Кључне речи: нуклеарни реактор, језгро реактора, канал реактора, горивна плоча, критична брзина, топлотни флукс